Reprinted from the Journal of the American Chemical Society, 1994, *116*.

Structural Preferences of Hydrogen-Bonded Networks in Organic Solution—the Cyclic $CA_3 \cdot M_3$ "Rosette"

John P. Mathias, Eric E. Simanek, Jonathan A. Zerkowski, Christopher T. Seto, and George M. Whitesides*

Contribution from the Department of Chemistry, Harvard University, Cambridge, Massachusetts 02138

Received September 29, 1993. Revised Manuscript Received February 27, 1994®

Abstract: Crystals grown from a solution containing equimolar portions of barbital (**3**) and *N,N'*-bis(4-*tert*-butylphenyl)-melamine (**4**) in toluene/isopropyl alcohol (1:1 v/v) comprise a cyclic $CA_3 \cdot M_3$ "rosette" (**5**). The six molecules in this supramolecular motif are held together by 18 hydrogen bonds. Characterization of *solutions* of equimolar mixtures of **3** and **4** in chloroform by ^1H NMR spectroscopy, gel permeation chromatography, and vapor pressure osmometry demonstrates that the same cyclic $CA_3 \cdot M_3$ rosette (**5**) is also the most probable structure, when [**3**] = [**4**] > 4 mM. ^1H NMR exchange experiments confirm that the $CA_3 \cdot M_3$ rosette (**5**) is qualitatively much less stable in chloroform solution than the supramolecular aggregate hub$(M)_3$:3barbital (**1**) that is preorganized for self-assembly by a covalent tris(melamine) derivative. Complexes formed between **4** and different isocyanurates indicate that intermolecular interactions, as a consequence of the steric bulk of the substituents on these derivatives, favor the formation of the cyclic $CA_3 \cdot M_3$ rosette over competing linear hydrogen-bonded motifs. There is inferential evidence for formation of a complex of modest stability with composition $CA \cdot M_2$ when 2[**3**] = [**4**].

Introduction

The potential of molecular self-assembly for the preparation of large supramolecular aggregates depends on the identification of noncovalently stabilized structural motifs whose enthalpic driving force for self-assembly is sufficient to overcome the unfavorable entropic consequences associated with the aggregation of several components into a single supramolecular entity.[1-3] We have chosen to use hydrogen bonds as primary elements with which to form supramolecular aggregates, in order to take advantage of the extensive body of information concerning hydrogen-bonded aggregation in solution[4,5] and in the solid state.[6,7] The hydrogen-bonded CA·M lattice[8] is the template on which we have based the design of a family of self-assembled hydrogen-bonded aggregates that are stable in organic solution.[9-11] Covalent preorganization of three melamines into a "tripod" molecule has facilitated the self-assembly of supramolecular aggregates that are stabilized by cyclic $CA_3 \cdot M_3$ rosettes, such as those represented schematically by **1** and **2** (Figure 1). We have demonstrated that these aggregates are stable in chloroform solution and have characterized their structures by ^1H and ^{13}C NMR spectroscopies, gel permeation chromatography, vapor pressure osmometry, and UV spectrophotometry.[9-13] With one exception, we have not been able to grow crystals of these aggregates and, therefore, have not been able to characterize them by X-ray crystallography.[14] We have determined the X-ray structure of a cyclic rosette of composition $CA_3 \cdot M_3$ (Figure 2).[15] This $CA_3 \cdot M_3$ rosette

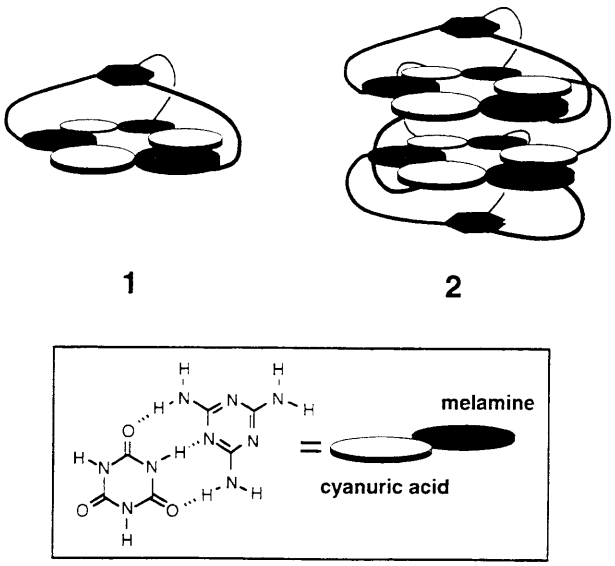

Figure 1. Schematic structures of two previously reported supramolecular aggregates based on $CA_3 \cdot M_3$ rosettes.

® Abstract published in *Advance ACS Abstracts*, April 1, 1994.

(1) Whitesides, G. M.; Mathias, J. P.; Seto, C. T. *Science* **1991**, *254*, 1312–1319.

(2) Lehn, J.-M. *Angew. Chem., Int. Ed. Engl.* **1990**, *29*, 1304–1319.

(3) Lindsey, J. S. *New J. Chem.* **1991**, *15*, 153–180. Baxter, P.; Lehn, J.-M.; DeCian, A.; Fischer, J. *Angew. Chem., Int. Ed. Engl.* **1993**, *32*, 69–72. Krämer, R.; Lehn, J.-M.; DeCian, A.; Fischer, J. *Angew. Chem., Int. Ed. Engl.* **1993**, *32*, 703–706. Copp, S. B.; Subramanian, S.; Zaworotko, M. J. *Angew. Chem., Int. Ed. Engl.* **1993**, *32*, 706–709. Ashton, P. R.; Bissel, R. A.; Spencer, N.; Stoddart, J. F.; Tolley, M. S. *Synlett.* **1992**, 914–918. Ashton, P. R.; Bissel, R. A.; Spencer, N.; Stoddart, J. F.; Tolley, M. S. *Synlett.* **1992**, 923–926. Constable, E. C. *Tetrahedron* **1992**, *48*, 10013–10059.

(4) For recent examples, see: Geib, S. J.; Vicent, C.; Fan, E.; Hamilton, A. D. *Angew. Chem., Int. Ed. Engl.* **1993**, *32*, 119–121. Fan, E.; Van Arman, S. A.; Kincaid, S.; Hamilton, A. D. *J. Am. Chem. Soc.* **1993**, *115*, 369–370. Yang, J.; Fan, E.; Geib, S. J.; Hamilton, A. D. *J. Am. Chem. Soc.* **1993**, *115*, 5314–5315. Bonazzi, S.; DeMorais, M. M.; Gottarelli, G.; Mariani, P.; Spada, G. P. *Angew. Chem., Int. Ed. Engl.* **1993**, *32*, 248–250. Boner-Law, R. P.; Sanders, J. K. M. *Tetrahedron Lett.* **1993**, *34*, 1677–1680. Mascal, M.; Moody, C. J.; Morrell, A. I.; Slawin, A. M. Z.; Williams, D. J. *J. Am. Chem. Soc.* **1993**, *115*, 813–814. Yoon, S. S.; Still, W. C. *J. Am. Chem. Soc.* **1993**, *115*, 823–824. Liang, G.-B.; Desper, J. M.; Gellman, S. H. *J. Am. Chem. Soc.* **1993**, *115*, 925–938.

(5) Zimmerman, S. C.; Duerr, B. F. *J. Org. Chem.* **1992**, *57*, 2215–2217.

(6) Desiraju, G. R. *Crystal Engineering: The Design of Organic Solids*; Elsevier: New York, 1989; pp 115–173.

(7) Etter, M. C. *Acc. Chem. Res.* **1990**, *23*, 120–126.

(8) We have illustrated the structure of the CA·M lattice in previous papers, see ref 1. This structure is a putative one, however, and has not been established unequivocally by single-crystal X-ray crystallography. The X-ray crystal structure of (CA)·(M)·3HCl has been reported, see: Wang, Y.; Wei, B.; Wang, Q. J. *Crystallogr. Spectrosc. Res.* **1990**, *20*, 79–82.

(9) Seto, C. T.; Whitesides, G. M. *J. Am. Chem. Soc.* **1993**, *115*, 905–916.

(10) Seto, C. T.; Mathias, J. P.; Whitesides, G. M. *J. Am. Chem. Soc.* **1993**, *115*, 1321–1329.

(11) Seto, C. T.; Whitesides, G. M. *J. Am. Chem. Soc.* **1993**, *115*, 1330–1340.

(12) Seto, C. T.; Whitesides, G. M. *J. Am. Chem. Soc.* **1990**, *112*, 6409–6410.

(13) Seto, C. T.; Whitesides, G. M. *J. Am. Chem. Soc.* **1991**, *113*, 712–713.

0002-7863/94/1516-4316$04.50/0

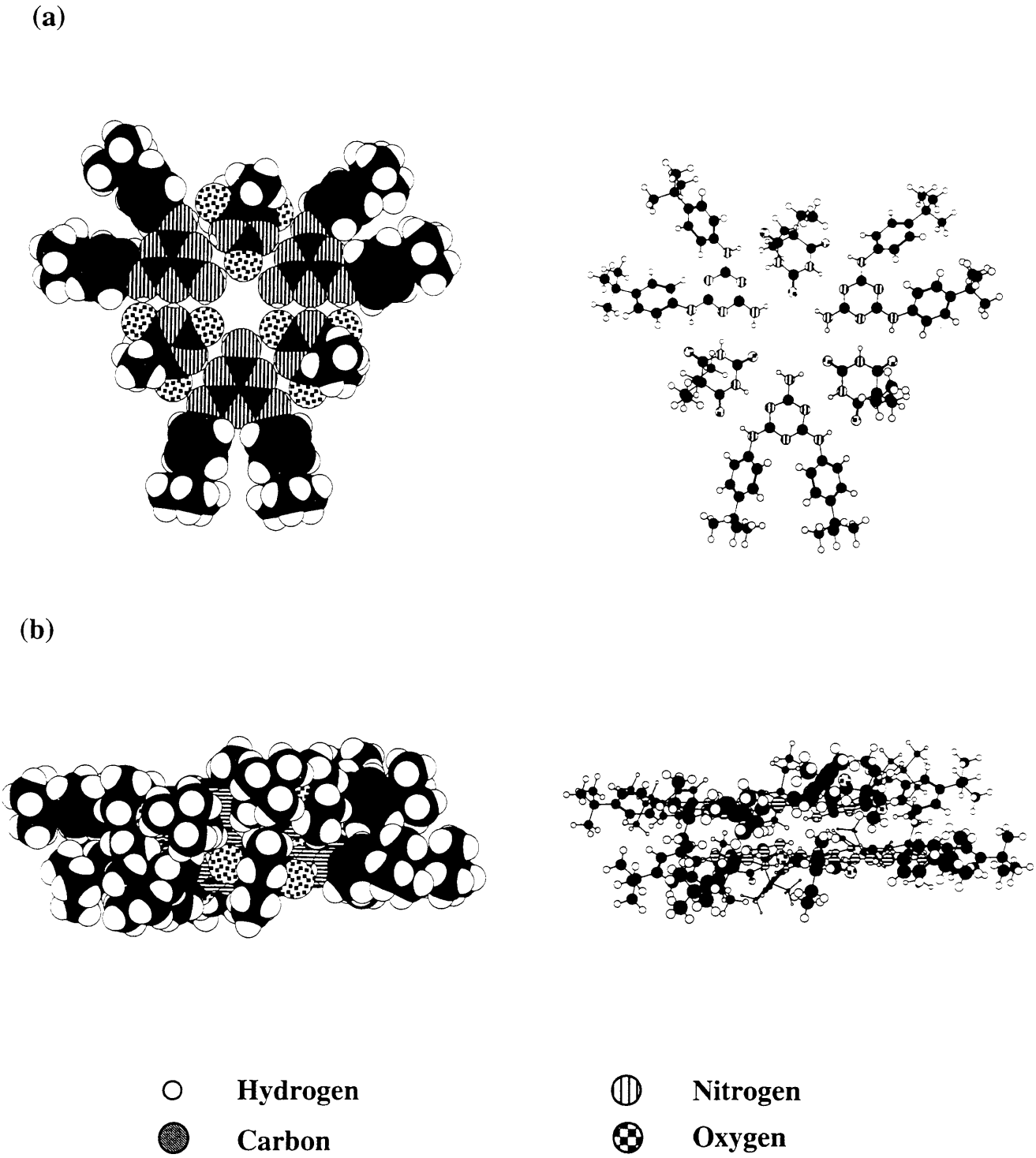

Figure 2. (a) X-ray crystal structure and (b) packing of the CA_3·M_3 rosette **5** formed between equimolar portions of **3** and **4** in van der Waal's surface and ball-and-stick representations.

(**5**) incorporates barbital (**3**) and *N,N'*-bis(4-*tert*-butylphenyl)-melamine (**4**) (Scheme 1). The finite cyclic CA_3·M_3 rosette is only one of many possible hydrogen-bonded motifs that could be adopted in the solid state by an equimolar mixture of **3** and **4**. We have, for example, seen two infinite hydrogen-bonded motifs, a linear tape and a crinkled tape, in 1:1 cocrystals between barbital and a number of disubstituted melamine derivatives.[16-19] These three motifs are shown together in Figure 3. Progression from one motif to another occurs as a consequence of the intermolecular steric interactions that occur between the substituents on the melamine and barbiturate derivatives. Intermolecular steric interaction between the substituents on adjacent melamines (linear tape), and also between the substituents on proximal melamine and barbiturate molecules (crinkled tape), are greater in these tape motifs than in the cyclic rosette. The regions of potential intermolecular steric overlap between substituents in each of these motifs are indicated on Figure 3. The steric bulk of the two *p-tert*-butylphenyl substituents in **4** is crucial in dictating the structural motif that is adopted in the cocrystal between **3** and

(14) Attempts to grow crystals of these aggregates that are suitable for X-ray crystallography have resulted in either amorphous powders or glasses.
(15) Zerkowski, J. A.; Seto, C. T.; Whitesides, G. M. *J. Am. Chem. Soc.* **1992**, *114*, 5473–5475.
(16) Zerkowski, J. A.; Seto, C. T.; Wierda, D. A.; Whitesides, G. M. *J. Am. Chem. Soc.* In press.
(17) Zerkowski, J. A.; Whitesides, G. M. *J. Am. Chem. Soc.* In press.
(18) Zerkowski, J. A.; Mathias, J. P.; Whitesides, G. M. *J. Am. Chem. Soc.* In press.
(19) Zerkowski, J. A.; Whitesides, G. M. *J. Am. Chem. Soc.* In press.

Scheme 1. Self-Assembly of the $CA_3 \cdot M_3$ Rosette

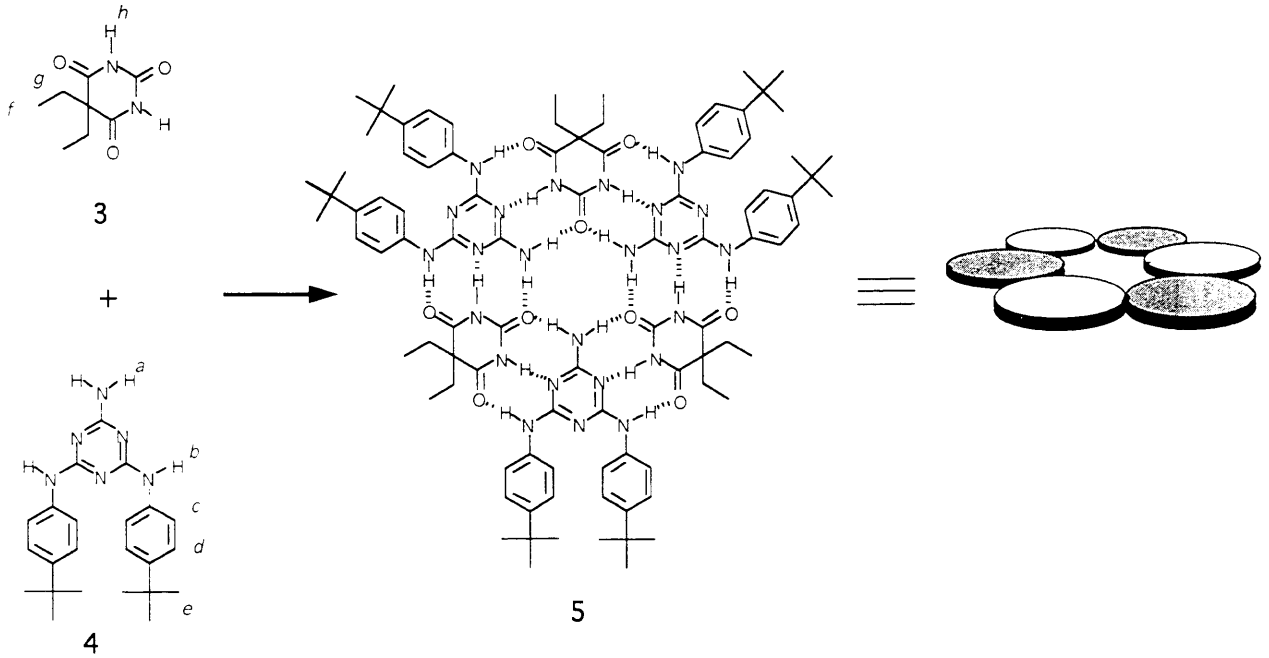

4. It is the $CA_3 \cdot M_3$ rosette that allows the sterically demanding groups on adjacent melamines to get as far away as possible from each other and from the ethyl substituents on the barbital ring.

In order to understand the occurrence and stability of the $CA_3 \cdot M_3$ rosette, we have examined the aggregates formed between barbital (3) and *N,N'*-bis(4-*tert*-butylphenyl)melamine (4) in both the solid state and in solution. The objectives of this study were (i) to assess whether the $CA_3 \cdot M_3$ rosette between 3 and 4 in the solid state was thermodynamically stable or kinetically determined, using X-ray powder diffraction and (ii) to determine the structural preference for the $CA_3 \cdot M_3$ rosette in solution using ^{1}H NMR spectroscopy, gel permeation chromatography, and vapor pressure osmometry. The results are beginning to define the structural preferences and stability of the $CA_3 \cdot M_3$ rosette—the basis for all of the self-assembled aggregates we have examined.

Results and Discussion

Assessing the Stability of the Cyclic $CA_3 \cdot M_3$ Rosette in the Solid-State by X-ray Powder Diffraction. Crystals of the 1:1 complex (5) formed between 3 and 4 grew on slow evaporation of a solution in isopropyl alcohol/toluene (~1:1 v/v). The structure of 5 in the solid state is shown in Figure 2.[15] The X-ray powder diffraction (XPD) pattern of 5 was calculated from this crystal structure (Figure 4a). We have used the calculated XPD pattern as the basis to search for other polymorphs of 5 in the solid state and, therefore, to infer the stability of the $CA_3 \cdot M_3$ rosette of 3 and 4, relative to tapes or other structures.[20,21]

Crystalline powders of 5 were obtained by recrystallization of an equimolar mixture of 3 and 4 from a variety of solvents. These powders were dried by evaporation at room temperature under atmospheric pressure (~2–5 days), ground, and subjected to XPD using X-rays from CuKα (λ = 1.54178 Å) with $3.6° < 2\theta < 33.6°$. XPD patterns for powders of 5 obtained from solutions in chloroform, acetone, acetonitrile, methanol/THF (1:1 v/v), and isopropyl alcohol/toluene (1:1 v/v: the solvent of crystallization) are illustrated in Figure 4b (traces i–v). The positions of the peaks in the XPD patterns from the various solvents and the calculated pattern are similar. Figure 4b (trace vi) shows the XPD pattern obtained after the powder from isopropyl alcohol/toluene (1:1 v/v) was annealed at 95 °C for 7 days. There are no significant changes in the positions of peaks or the overall pattern in the XPD picture after annealing this sample. The $CA_3 \cdot M_3$ rosette appears, therefore, to be a thermodynamically stable morphology.

From these observations by XPD, we conclude that the structure for the 1:1 complex between 3 and 4 in the solid state is independent of the solvent used for crystallization.[22] We infer that the self-assembly of the cyclic CA_3M_3 rosette reflects the formation of a stable cyclic aggregate of 3 and 4, rather than a kinetic artifact of rates of nucleation or crystal growth.

The 1:1 Complex Formed between 3 and 4 in Chloroform Is More Soluble Than 3 or 4 Alone. The solubilities of 3 and 4 in chloroform are low (<0.5 mM). Adding aliquots of 3 to 4 in chloroform, however, leads to the formation of a hydrogen-bonded supramolecular aggregate (5) that is highly soluble (>100 mM), once the relative proportions of 3 and 4 are 1:1. This significant increase in solubility of the molecules on aggregation in chloroform is also exhibited in the formation of self-assembled aggregates of types 1 and 2 (Figure 1).[9] In all of these cases, self-assembly of the $CA_3 \cdot M_3$ rosette allows the polar, hydrogen-bonding functionalities in the components to form soluble cyclic aggregates rather than extended insoluble networks. Small hydrogen-bonded linear oligomers formed between 3 and 4 would have large areas of polar functionality in contact with the solution. Indeed, the solubilities of 1:1 complexes between barbital (3) and other *N,N'*-bis(4-alkylphenyl)melamines with less bulky substituents are very low in chloroform (<2 mM). Even the 1:1 complex between barbital and *N,N'*-bis(4-isopropylphenyl)melamine has a solubility below 5 mM in chloroform. The high solubility of the 1:1 complex formed between 3 and 4 can, we believe, be interpreted as a consequence of self-assembly of the cyclic $CA_3 \cdot M_3$ rosette.

Assessing the Characteristics of the Cyclic $CA_3 \cdot M_3$ Rosette in Solution by ^{1}H NMR Spectroscopy. ^{1}H NMR spectra of solutions obtained by titration of a solid barbital (3) into a suspension of

(20) We have made many attempts to grow crystals from equimolar solutions of 3 and 4 from other solvents and to search for other polymorphs directly by X-ray crystallography, without success. In these cases, the smallest dimensions of any single crystals obtained was less than 0.05 mm.

(21) We have previously inferred the existence of different morphologies for 1:1 mixtures of melamines and barbiturates using XPD, see ref 16. Confirmation of these different morphologies was then provided by ^{13}C solid-state NMR—Wazeer, M.; McDonald, J.; Weisbecker, C.; Whitesides, G. M. Unpublished results.

(22) The positions of the major peaks in the pattern obtained from chloroform coincide with those in the calculated pattern. Although there is an absence of peaks in new positions and or shifting in the position of peaks from the calculated pattern there does, however, appear to be a broadening and loss of resolution in the pattern. We do not rule out the presence of other polymorphs or minor impurities to account for this phenomena.

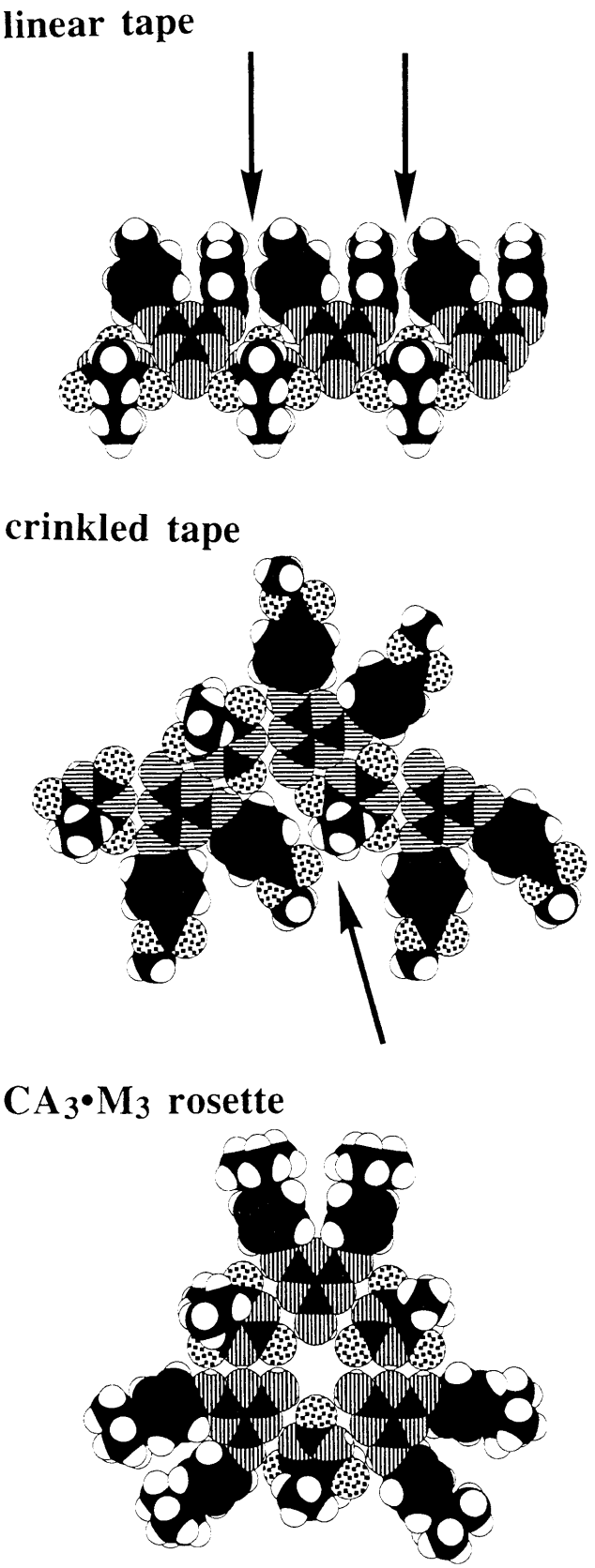

Figure 3. Crystallographic structures of the three hydrogen-bonded motifs observed in cocrystals between derivatives of barbituric acid and *N,N'*-disubstituted melamine. They are the linear tape (top), the crinkled tape (middle), and the CA_3-M_3 rosette (bottom). Regions of intermolecular steric interaction between the substituents on adjacent melamine rings in the linear tape and between the substituents on melamine rings and proximal barbiturates in the crinkled tape motifs are indicated by arrows.

N,N'-bis(4-*tert*-butylphenyl)melamine (**4**) in $CDCl_3$ are illustrated in Figure 5a–d (the nominal concentration of **4** was 7 mM). Annotation of these spectra refer to the labels on **3** and

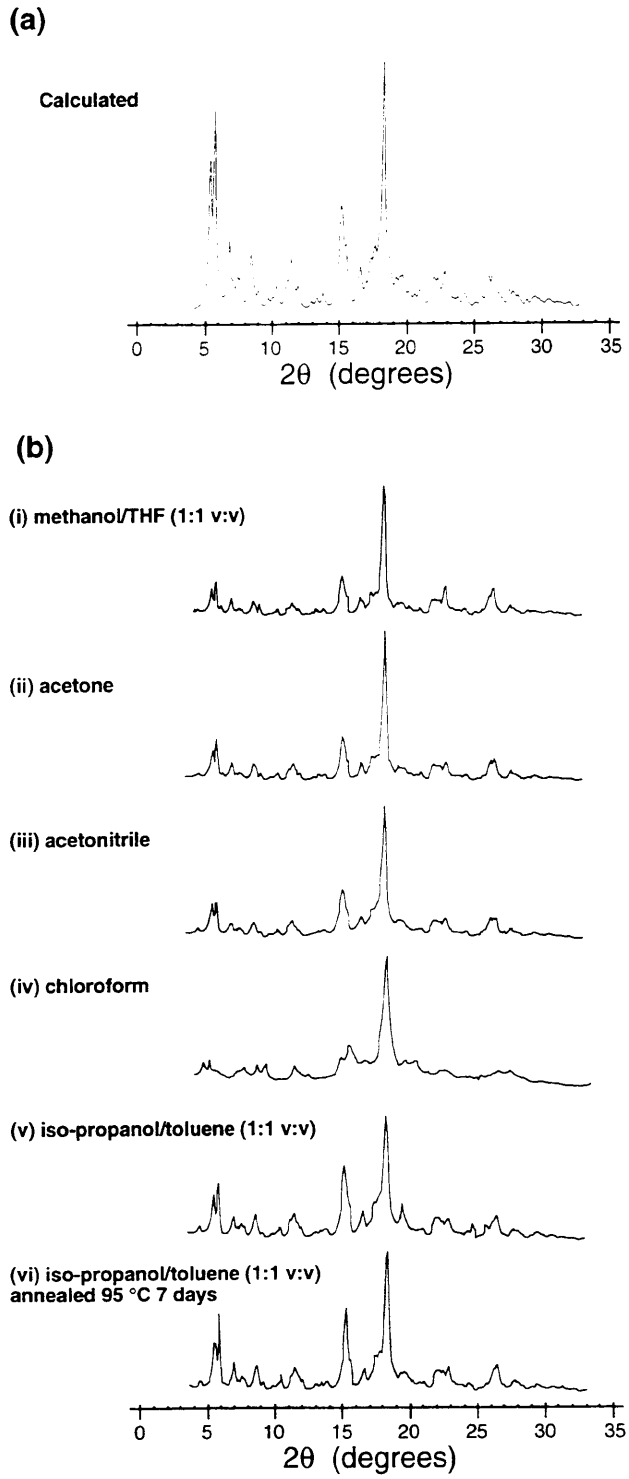

Figure 4. (a) Calculated XPD pattern for the CA_3-M_3 rosette **5**. (b) Patterns obtained from XPD on samples of **5** formed by crystallization from different solvents.

4 in Scheme 1. Addition of barbital solubilizes **4** until 1:1 stoichiometry is reached. At this stoichiometry, the solution becomes homogeneous. Further aliquots of barbital remain insoluble.

During this titration, the chemical shift of the NH_2 protons (H^a) on the melamine derivative **4** moves downfield from 5.45 to 7.15 ppm. The chemical shift of the NH protons (H^b) on **4** moves downfield from 7.25 to 9.60 ppm. The changes in chemical shift for H^a and H^b on addition of barbital suggest that they are involved in strong hydrogen bonding. One set of phenyl protons (H^c) on **4** also moves downfield from 7.45 to 7.60 ppm during the titration. The hydrogen-bonded imide protons on barbital (H^h) in the 1:1 aggregate appear as a broad signal at δ 14.1 ppm.[23,24]

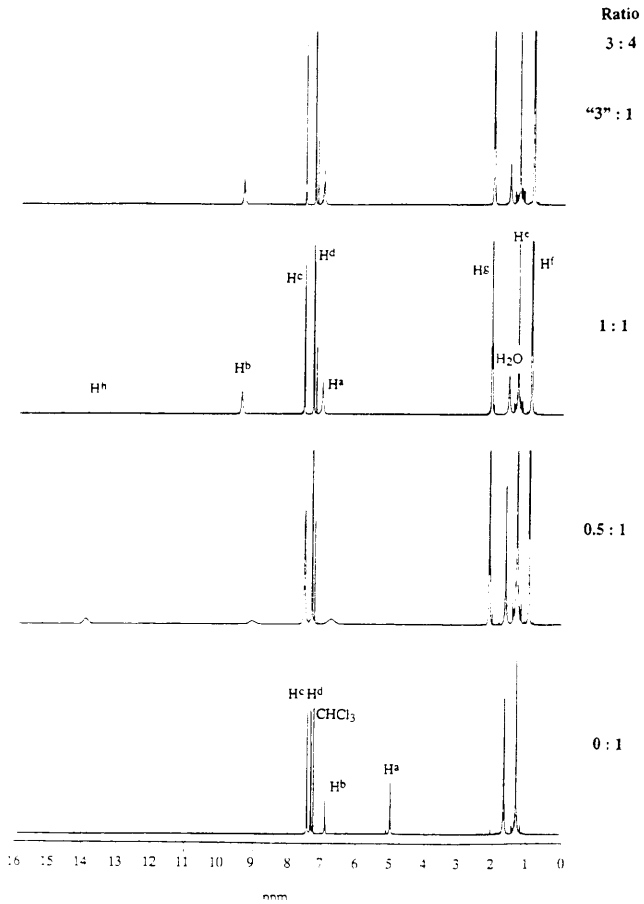

Figure 5. ^{1}H NMR spectra of a titration between **3** and **4** (500 MHz, $CDCl_3$). Solid **3** was added to a suspension of **4** and heated to reflux to afford a homogeneous solution. Annotations refer to those indicated on Scheme 1. The resonance for the isocyanurate protons H^h is broadened into the base line in the $CA_3{\cdot}M_3$ rosette.

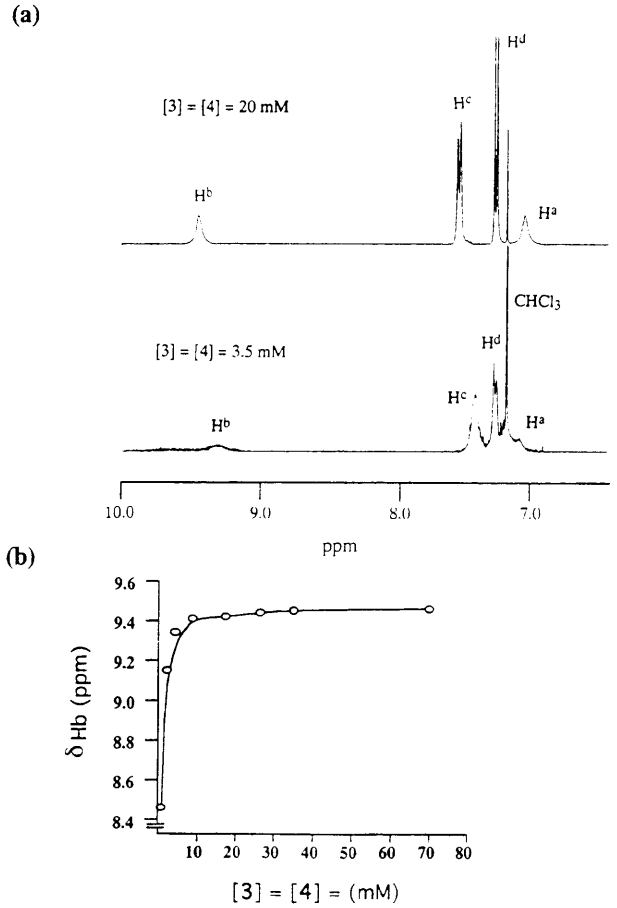

Figure 6. (a) Partial ^{1}H NMR spectra for **5** taken at [**3**] = [**4**] = 20 mM and [**3**] = [**4**] = 3.5 mM concentrations. (b) Plot of the chemical shift of H^b on the melamine derivative **4** against concentration. Annotations refer to those in Scheme 1.

The absence of separate peaks associated with "bound" and "free" components in this titration suggests that exchange between complexes and uncomplexed states is fast on the NMR time scale, at room temperature. This rapid exchange observed for **5** contrasts to that observed for aggregates of type **1** and **2** (Figure 1): exchange between bound and unbound states in these aggregates is slow on the NMR time scale; both states are clearly visible.[9-11] The aggregate **5** therefore exhibits more rapid exchange of bound and free components than does the covalently preorganized aggregates **1** and **2**.

The effects of concentration on the chemical shift of the melamine NH protons (H^b) in **5** are illustrated in Figure 6. Little change occurs as a solution of **5** in chloroform is diluted from [**3**] = [**4**] = 70 to 4 mM (Figure 6a). Below [**3**] = [**4**] = 4 mM, a sharp upfield shift is seen for H^b, and the resolution of the spectra decreases sharply (Figure 6b). The curve obtained for δH^b vs [concn] from these data (Figure 6c) suggests that the degree of hydrogen bonding is insensitive to concentration when [**3**] = [**4**] > 4 mM and, therefore, that the assembly/disassembly of the complex formed between **3** and **4** displays positive cooperativity once this concentration is reached.[25] The degree of hydrogen bonding should change more steadily as a function of concentration for noncooperative association. When [**3**] = [**4**] < 4 mM, the degree of hydrogen bonding is very sensitive to changes in concentration. The concentration-dependent aggregation seen for **5** by ^{1}H NMR in $CDCl_3$ correlates strongly with that observed by VPO (see later).

Figure 7 shows the changes in the ^{1}H NMR spectrum of a solution of **5** in chloroform that occur with temperature. These variable temperature NMR experiments were performed with concentrations [**3**] = [**4**] = 3 mM in $CDCl_3$. This concentration is below that required to give a well defined aggregate, and there is, therefore, little detail in the NMR spectrum at room temperature. In this experiment, we hoped to see the transition from a poorly defined mixture of rapidly equilibrating structures at higher temperature to separate, more ordered structures as the rate of exchange was reduced at progressively lower temperatures.

Decreasing the temperature from 293 to 226 K did sharpen the resonances. At 293 K the chemical shifts of the phenyl protons (H^3/H^d, δ 7.30 and 7.45, respectively) are close to those observed for **4** in chloroform. Resonances for the melamine protons H^a and H^b also appear as broad signals that are upfield, relative to their position in **5**. The barbiturate protons H^h (not shown) are broadened completely into the base line. As the temperature decreases, the progression to the fully assembled $CA_3{\cdot}M_3$ rosette is apparent, until at 226 K, H^c/H^d appear predominantly (>90%) as two sharp signals at δ 7.30 and 7.60, respectively, and the chemical shifts and peak shapes of all other protons correspond to those seen in the fully bound 1:1 complex **5** (Figure 5a). NOE effects in related systems have confirmed that the melamine protons H_c *do* correspond to the doublet that is farthest downfield, δ 7.60 ppm in **5**, relative to H^d at δ 7.30 ppm. At higher temperatures the doublet for the aromatic protons H^c displays broadening, probably as a consequence of exchange between the fully-assembled state and several different partially assembled states. At 226 K, the rate of exchange between states is slow enough to see the individual components and the majority of H^c

(23) The chemical shift of the barbiturate protons (H^h) in DMSO is δ 11.2 ppm; in 5% DMSO/$CHCl_3$ (v/v) it is 10.9 ppm.

(24) The appearance of H^h as a broad signal in **5** contrasts with observations made on previously reported supramolecular aggregates such as **1** and **2**, and, indeed, with many of the other $CA_3{\cdot}M_3$ rosettes reported in Scheme 4 later in this paper. In all of these cases, the hydrogen-bonded isocyanurate/barbiturate protons appear as sharp signals in the region 14–16 ppm in $CDCl_3$.

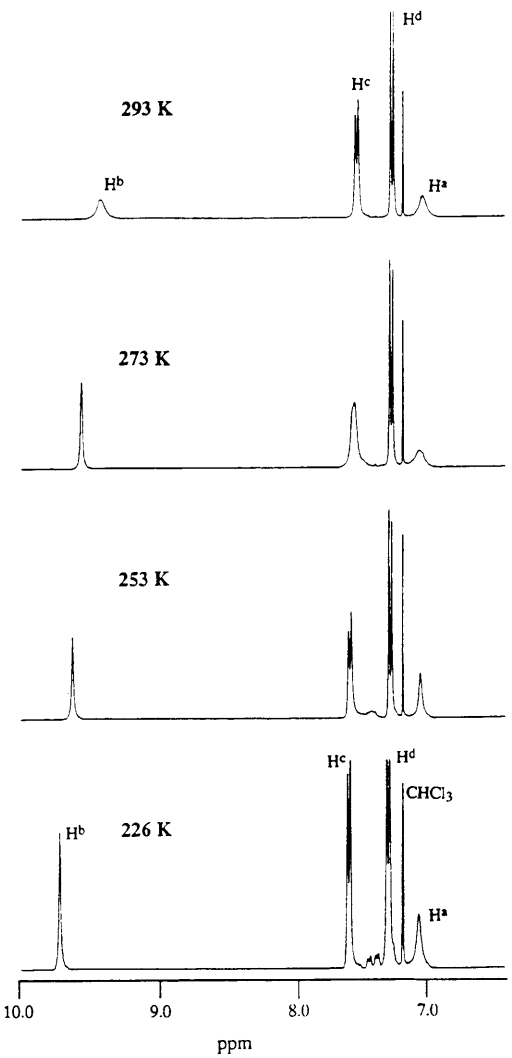

Figure 7. Spectra obtained from variable temperature ^{1}H NMR on the aggregate **5** at a concentration of [**3**] = [**4**] = 3 mM, with respect to the components (400 MHz, $CDCl_3$). Annotations refer to those in Scheme 1.

appears as a doublet at δ 7.60 ppm, corresponding to the fully-assembled rosette **5**. Other aggregates are visible as two small doublets at approximately δ 7.4 ppm. The differences in line broadening between H^c and H^d at 273 K suggest that both of these doublets are due to H^c and that the corresponding doublets for H^d are incorporated into the single doublet observed. The difference in the behavior of H^c and H^d during the cooling of this solution is a consequence of the closer proximity of H^c than H^d to the hydrogen bonding sites. While H^d will also undergo exchange, this position is not close enough to the hydrogen-bonded region to experience a significant change in its environment and, therefore, in its chemical shift during complexation and decomplexation.

The data from variable-temperature NMR spectroscopy suggest that the 1:1 complex formed between **3** and **4** (at 4 mM) is present predominantly (>90%) as the single hydrogen-bonded structure represented by the cyclic CA_3·M_3 rosette (**5**) at 226 K. They also suggest that the remaining material is present in other hydrogen bonded forms—perhaps smaller linear oligomers?

Assessing the Characteristics of the Cyclic CA_3·M_3 Rosette in Solution by Gel Permeation Chromatography (GPC). Gel permeation chromatography can be used to examine the heterogeneity and relative stabilities of hydrogen-bonded self-assembled aggregates in solution.[26,27] The kinetic stability of a complex must, however, be sufficient for it to elute intact. We have demonstrated that complexes of types **1** and **2** (Figure 1) are stable enough to be characterized by GPC.[9-11] Complexes of type **1**, however, dissociate significantly during the 7–10 min required for analysis. As a result, their peaks exhibit tailing.

Examination of the 1:1 complex formed between **3** and **4** by GPC (eluting with $CHCl_3$) shows no evidence for a supramolecular aggregate that is stable enough to pass through the GPC column without dissociation. While **3** is sufficiently insoluble that it does not elute off the column alone, **4** elutes from the column after xylenes as a broadened peak suggesting that it absorbs to the column matrix. Mixtures of [**3**] = [**4**] do not elute from the column before the xylenes marker. The low solubility of both components in chloroform precluded running an experiment in which the eluent was a solution of either component in chloroform, so that dissociation of the rosette during analysis would no longer be an irreversible process.

Characterizing the CA_3·M_3 Rosette by Vapor Pressure Osmometry (VPO). The 1:1 complex formed between barbital (**3**) and *N,N'*-bis(4-*tert*-butylphenyl)melamine (**4**) was examined by VPO over the concentration range 0.5–32 mM (all concentrations refer to those of the individual components, not of the putative CA_3·M_3 rosette). The plot of ΔV·[**3** or **4**]$^{-1}$ vs [**3** or **4**] obtained from VPO is shown in Figure 8a. The curvature of this plot shows that **5** displays nonideal behavior in solution at concentrations below ~4 mM. Data obtained from a self-assembled aggregate of type **1**—hubM_3:3*neo*hex(CA)—and the cyclic decapeptide *N,N'*-bis(^{t}Boc)-gramicidin S are included in Figure 8a for reference.[28] Both hubM_3:3*neo*hex(CA) and *N,N'*-bis-(^{t}Boc)-gramicidin S give straight lines in the plot of ΔV·[**3** or **4**]$^{-1}$ vs [**3** or **4**] that show a slight negative slope as the concentration increases. We have proposed that this feature is a result of concentration-dependent aggregation (both structures have hydrogen bond donors and acceptors on their periphery).[9] Aggregation causes the actual number of particles in solution to decrease. The *change in vapor pressure* sensed by osmometry is, therefore, smaller than would be expected under ideal conditions. Thus, the ratio of ΔV·[**3** or **4**]$^{-i}$ vs [**3** or **4**] decreases, resulting in a negative slope to the plot.

At concentrations [**3**] = [**4**] > 4 mM (2.5 g/L), the behavior of **5** is similar to that of hubM_3:3*neo*hex(CA) and *N,N'*-bis-(*tBoc*)-gramicidin S. Analysis of the data from three separate experiments for **5** over the range 4–32 mM (Figure 8a; inset) gives the apparent molecular weights for the aggregate in solution shown in Figure 8b, when compared against four different standards of known molecular weight. The calculated molecular weight for the cyclic CA_3·M_3 rosette **5** is 1.72 kDa. While the use of many molecular weight standards leads to a distribution of observed molecular weights for the unknown sample, it decreases the bias caused by any nonideal behavior of the standards. The agreement between the observed molecular weight and the value calculated for the cyclic CA_3·M_3 rosette **5** lead us to conclude that this motif is the most probable structure for the 1:1 complex between **3** and **4** in solution, at concentrations when [**3**] = [**4**] > mM.

Data from the equimolar mixture when [**3**] = [**4**] < 4 mM exhibit a highly negative slope. This observation is consistent with an increasing degree of aggregation between the molecules as the concentration increases in this range. We believe that the components **3** and **4** are present in solution in a mixture of states including **5**, the uncomplexed components, and larger hydrogen-bonded oligomers when [**3**] = [**4**] < 4 mM. Treatment of these data suggest the average molecular weight of any aggregates in solution below 4 mM is in the range 0.5–0.8 kDa (FW_3 184, FW_4

(25) Similar observations have been made, and conclusions drawn, concerning the self-assembly of a hydrogen-bonded trimer by Zimmerman, see ref 5.

(26) Part C, Polymer Symposia 21. In *Journal of Polymer Science*; Johnson, J. F., Ed.; 1968; pp 1–344.

(27) Stevens, F. J. *Biochemistry* **1986**, *25*, 981–993. Stevens, F. J. *Biophysics J.* **1989**, *55*, 1155–1167.

(28) Original data from VPO for hubM_3:3*neo*hex(CA) and *N,N'*-bis-(^{t}Boc)-gramicidin S were reported in ref 9.

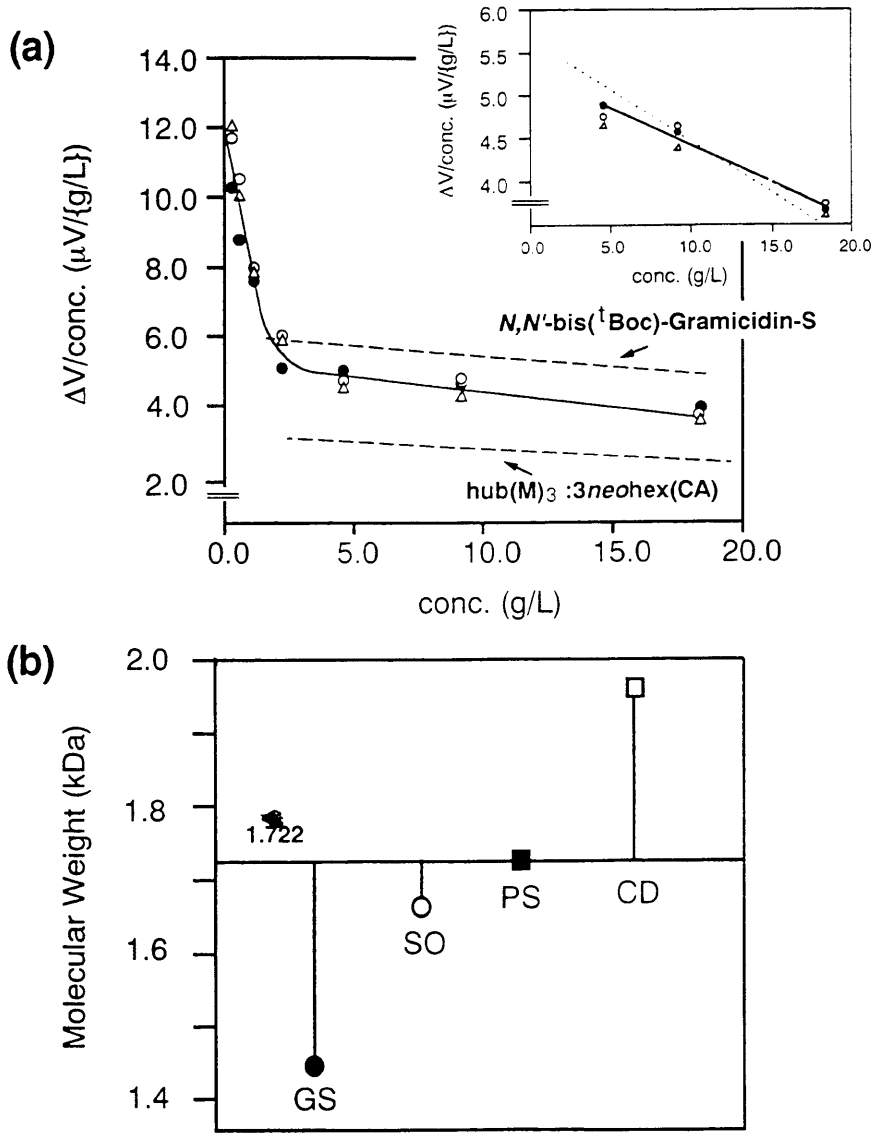

Figure 8. Estimation of the molecular weight in solution of rosette **5** by vapor pressure osmometry. (a) Concentration dependence of data from VPO for the equimolar mixture of **3** and **4** over the range [**3**] = [**4**] = 0.5–32 mM. Results from three separate experiments (○, △, and ●) are shown. The solid line joining these data is provided as a guide to the eye. The dashed lines illustrate concentration dependence of data from a self-assembled aggregate, hub(M)$_3$:*neo*hex(CA) and the cyclic decapeptide *N,N*-bis(^{t}Boc)-gramicidin S. The inset shows a plot of the same data over the range 4–32 mM (three experiments). These data were used to calculate the molecular weight for **5** in chloroform. (b) Observed molecular weights for **5**. The solid horizontal bar and associated number represent the calculated molecular weight of the cyclic CA$_3$·M$_3$ rosette. Measurements were correlated against four different molecular weight standards: *N,N'*-bis(^{t}Boc)-gramicidin-S (FW 1342) (●), sucrose octaacetate (FW 679) (○), polystyrene (av FW 5050, polydispersity 1.05) (■), and perbenzoyl-β-cyclodextrin (FW 3321) (□). Measurements were made in chloroform at 37 °C.

390). The concentration dependent behavior when [**3**] = [**4**] < 4 mM observed for **5** in VPO correlates strongly with that witnessed by ^{1}H NMR spectroscopy.

Evidence for an Aggregate of Composition CA·M$_2$ when 2[3] = [4]. An anomaly in Figure 5 is the appearance of a signal for H^h at 2[**3**] = [**4**] and its disappearance at [**3**] = [**4**]. We have explored this feature further and believe that 2[**3**] = [**4**] probably arises from the trimer **7** with structure CA·M$_2$ (Scheme 2). The very low solubility (<0.5 mM) of **3** and the presence of hydrogen-bonded imide protons suggests that *all* **3** is in association with at least 1 equiv of **4**. Three hypothetical structures result (**6**–**8**). The low solubility of **4** favors **7** over **6** and **8**. Additional evidence from ^{1}H NMR that favors **7** over **6** and **8** is the absence of aromatic signals for free **4** when 2[**3**] = [**4**]. If **8** were present in the mixture, a well-resolved imide resonance H^h derived from the rosette should be equally well-resolved in [**3**] = [**4**].

VPO indicates that the average molecular weight of the species present when 2[**3**] = [**4**] is between MW 450 and 700. The MW of **7** is 964 (FW$_3$ = 184, FW$_4$ = 390). A disparity between calculated MW and that obtained through VPO measurements is not uncommon, and although the discrepancy between calculated and experimental MW is unusually large, these values for 2[**3**] = [**4**] *are* different than those calculated for [**3**] = [**4**] which varied from 1450 to 1950 (MW for **5** is 1722). The number-averaged molecular weights for **6** and **8** are calculated to be 482 and 721.

Removal of solvent by evaporation from a THF/MeOH solution with 2[**3**] = [**4**] and analysis by XPD of the resulting solid reveals a PD pattern that is the superposition of uncomplexed melamine and rosette. This observation reinforces our belief that the rosette motif is a favorable architecture in the solid state.

We believe that the appearance of a resolved H^h resonance for **7** and its absence in **5** is a result of the relative dynamic behaviors of these aggregates. One inference from these line shapes is that **7** is more slowly exchanging than **5**. We cannot presently rationalize these relative stabilities.

The NH resonances (H^a and H^b) of the melamines of the rosette are better resolved than those of the trimer. This difference is in the opposite sense than what is observed for the barbiturate H^h. Two points must be considered. First, the width of the peaks due to H^a and H^b in the trimer are the average of hydrogen bonded and nonbonded protons. Second, imide protons are much

Scheme 2. Hypothetical Structures Resulting from 2[3] = [4][a]

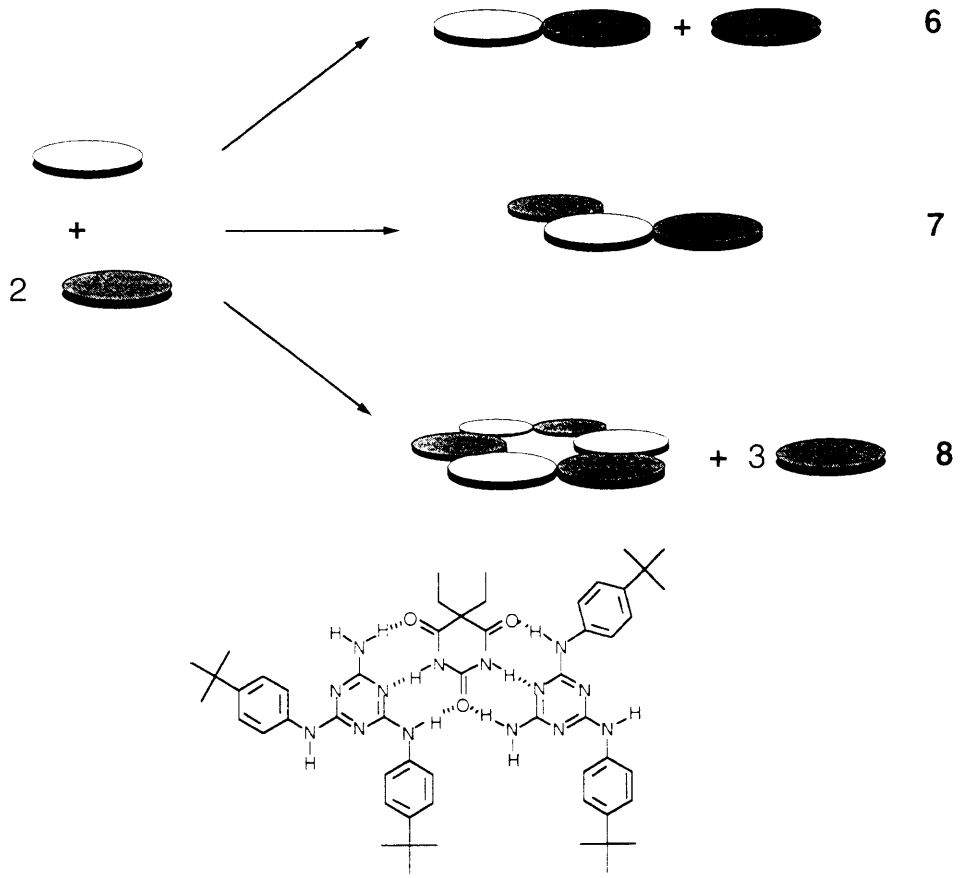

[a] One of a number of isomers of composition CA·M_2 is indicated; the positions and relative stereochemistries of the phenyl groups in the system we have studied is not defined by the available information.

more sensitive to environment than are the NH protons of the melamines.[29]

Assessing the Relative Stabilities of the CA_3·M_3 Rosette and a Covalently Preorganized Aggregate Hub(M)$_3$:3barbital. The exchange experiment illustrated in Scheme 3 was performed to assess the *relative* stabilities of the CA_3·M_3 rosette **5** (six components, preorganized by steric interactions between substituents) and the supramolecular aggregate hub(M)$_3$:3barbital **10** (four components, preorganized by covalent bonding). The failure to observe the rosette **5** by GPC indicates that this aggregate is substantially less stable than **10**. A solution of **5** in $CDCl_3$ (10 μmol of each component, **3** and **4**, in 1 mL) was treated with uncomplexed hub(M)$_3$ (3.3 μmol) and incubated in an NMR tube at 25 °C for 7 days.[30] Exchange of the barbital from the CA_3·M_3 rosette to the aggregate **10** was complete, as judged by ^{1}H NMR. This observation confirms that the thermodynamic stability of **5** is lower than that of **10** but does not permit a quantitative estimate of the eqiulibrium constant. Incubation of a solution of **10** with 3 equiv of *N,N'*-bis(*p-tert*-butylphenyl)-melamine **4** had no effect on the ^{1}H NMR spectrum. No exchange was observed.[31]

The Generality of the CA_3·M_3 Rosette Motif in Solution. Scheme 4 summarizes the different combinations of components that afford a cyclic CA_3·M_3 rosette in solution, as judged by ^{1}H NMR.[32] These results demonstrate that the steric bulk of the *p-tert*-butylphenyl substituent on **4** is the key feature that favors formation of the CA_3·M_3 rosette between **3** and *N,N'*-bis(4-alkylphenyl)melamine. Formation of the cyclic CA_3·M_3 rosette appears to be a more general feature, however, of complexation between *N,N'*-bis(4-*tert*-butylphenyl)melamine **4** and sterically demanding isocyanurates. The steric bulk of the substituents in 3,3,3-triphenylpropylisocyanurate **12** also appears to favor formation of the CA_3·M_3 rosette strongly, even with less sterically hindered derivatives of melamine.[33]

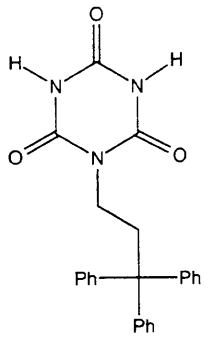

12

Conclusions

The cyclic CA_3·M_3 rosette (**5**) appears to be the stable 1:1 complex between barbital (**3**) and *N,N'*-bis(*p-tert*-butylphenyl)-melamine (**4**) in the solid state. Indeed, the cyclic CA_3·M_3 motif is the only morphology observed in the solid state by XPD. Data

(29) The ^{1}H NMR spectrum at low temperatures of aggregates of structure **1** show that the chemical shifts for imide resonances occur between 13 and 16 ppm. The N–H resonances, however, often appear with very similar chemical shifts. A similar observation has been made with aggregates similar to **5** based on asymmetric melamines.

(30) Exchange is certainly complete in a much shorter interval.

(31) These indictions of the relative stabilities of **5** and **10** are, therefore, in agreement with the predictions suggested by the behavior of the aggregates under analysis by GPC.

(32) The syntheses of **11** and **12** are reported in ref 9. Those for **13** and **14** are reported in ref 16, and that for **15** is reported in ref 18.

(33) The synthesis and characterization of **12** is reported in ref 9.

(34) Mathias, J. P.; Simanek, E. E.; Whitesides, G. M. *J. Am. Chem. Soc.*, following paper in this issue.

Scheme 3. Exchange Experiment To Assess the Relative Stabilities of the Self-Assembled Aggregates **5** and **10**

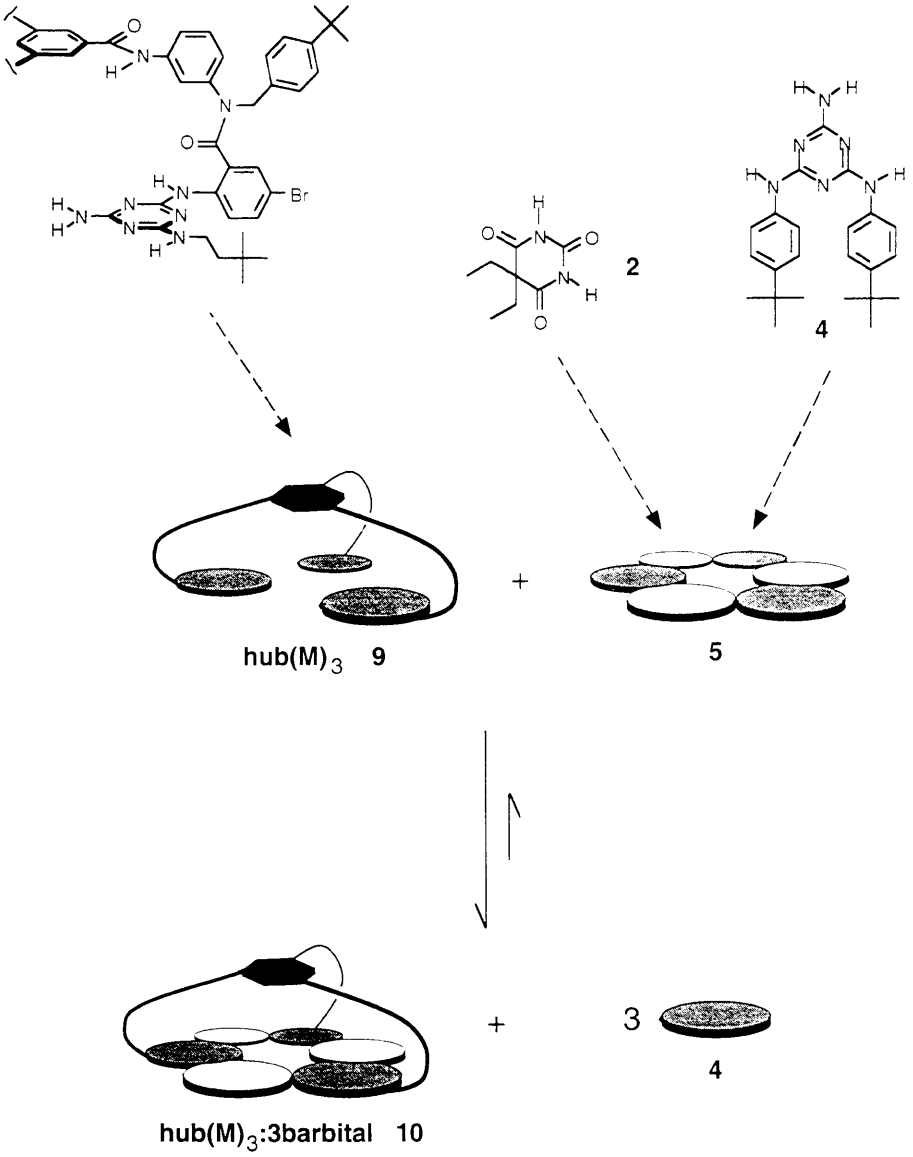

from solution, when taken together, indicate that the $CA_3{\cdot}M_3$ rosette is the major species present in equimolar mixtures of **3** and **4** in chloroform solution at concentrations greater than ~4 mM.

Studies by NMR and VPO establish that the self-assembly of the $CA_3{\cdot}M_3$ rosette between **3** and **4** is concentration dependent. Below 4 mM, the components **3** and **4** are present as an equilibrating mixture of linear structures (probably containing two or three of both **3** and **4**). Above this concentration, the hydrogen-bonded aggregate is insensitive to concentration.

The $CA_3{\cdot}M_3$ rosette is less stable than aggregates of type **1** and **2**, as judged by GPC. This finding has been confirmed by the direct competition experiments performed between the $CA_3{\cdot}M_3$ rosette **5** and the self-assembled aggregate **10**. These experiments demonstrate that **10** has greater thermodynamic stability than **5**.

The stability of **5** is too low to be interesting, by itself, as a building block for supramolecular chemistry. As the common structural motif for all of the more complex structures we have generated, it is interesting as the simpliest aggregate of its class. We emphasize the $CA_3{\cdot}M_3$ rosette **5** displays a surprisingly *high* degree of stability for a supramolecular aggregate that is composed of six particles and stabilized by only 18 hydrogen bonds. Complexes of cyanuric acid and melamine with smaller substituents do *not* form well-defined rosettes, in solution or in the solid state. These observations indicate that intermolecular steric interactions around the periphery of the rosette can be used to assist self-assembly of supramolecular aggregates. The data presented in Scheme 4 reinforce the notion that steric crowding around the periphery of the self-assembled aggregates may be used to select the $CA_3{\cdot}M_3$ rosette in preference to other hydrogen bonded motifs in this series of self-assembled aggregates. Peripheral steric crowding could, therefore, represent an alternative or supplemental strategy for the preparation of self-assembled aggregates based on the $CA_3{\cdot}M_3$ rosette, without the need for covalent preorganization. The validity of this hypothesis, and the development of strategies to increase the stability of such supramolecular aggregates, are discussed in the following paper in this issue.[34]

Experimental Section

X-ray Powder Diffraction. Crystals of the 1:1 complexes were obtained as the homogeneous solutions cooled to room temperature, filtered, dried, and ground with an agate mortar and pestle. The resulting powder was placed in the well of a fiberboard sample holder, and the surface of the powder was pressed flat with a spatula. Scans were performed from 3.6° to 33.6° in 2θ, counting 30 s at each step of 0.1°, on a Philips powder diffractometer.

NMR Spectroscopy. NMR experiments were performed with a Bruker AM 500 instrument. The NOE spectra of these supramolecular aggregates were recorded at 25 °C, with an evolution period of 3.0 s and

Scheme 4. Effect of Different Substituents on the Self-Assembly of the CA_3·M_3 Rosette in Chloroform, as Judged by ^{1}H NMR Spectroscopy[a]

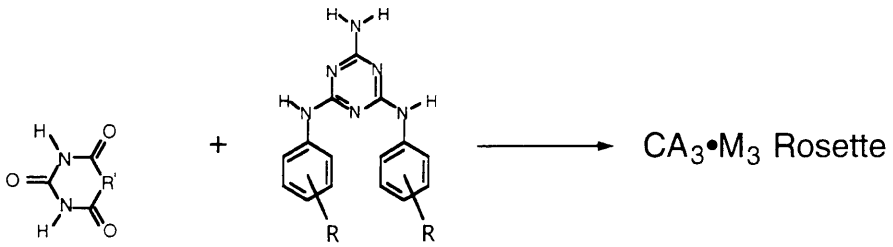

R'		R		Rosette ?
CEt_2	(3)	*p*- Me	(13)	No
CEt_2	(3)	*p*-^{i}Pr	(14)	No
$NCH_2CH_2C(Me)_3$	(11)	*p*-^{t}Bu	(4)	No
CEt_2	(3)	*p*-^{t}Bu	(4)	Yes
$NCH_2CH_2C(Ph)_3$	(12)	*p*-^{t}Bu	(4)	Yes
$NCH_2CH_2C(Ph)_3$	(12)	*p*-Me	(15)	Yes
$NCH_2CH_2C(Ph)_3$	(12)	*m*-Me	(16)	Yes

[a] "Yes" indicates formation of a rosette; "No" indicates that formation of a rosette was not observed.

a relaxation delay of 6.0 s. The complex (5.0 μmol) was dissolved in 0.7 mL of $CDCl_3$, and the sample was degassed with five freeze–pump–thaw cycles.

Gel Permeation Chromatography. Gel permeation chromatography was performed using a Waters 600E HPLC with a Waters 484 UV detector and Waters analytical gel permeation column (Ultrastyragel, 1000Å pore size). Elutions were performed at room temperature using HPLC grade CH_2Cl_2 or $CHCl_3$ as the eluent at a flow rate of 1.0 mL/min. The injection volume was 20 μL.

Molecular Weight Determinations by Vapor Pressure Osmometry. Molecular weight determinations were made with a Wescan Model 233 vapor pressure osmometer operated at 35 °C. The molecular weight of the complexes were measured in HPLC grade glass distilled chloroform at concentrations of approximately 0.5, 1, 2, 4, 8, and 16 mM. At each concentration, 3–4 measurements were taken. Calibration curves were generated using four molecular weight standards: sucrose octaacetate (MW 679), perbenzoyl β-cyclodextrin (MW 3321), polystyrene (MW 5050, polydispersity = 1.05), and a derivative of gramacidin S in which the two ornithine amino groups had been converted to their *tert*-butylcarbamates (MW 1342).

Specific Procedures. *N,N*-Bis(4-*tert*-butylphenyl)melamine (4). Two equivalents of 4-*tert*-butylaniline (0.94 mL, 6.72 mmol) were added to a solution of cyanuric chloride (618 mg, 3.36 mmol) and diisopropylethylamine (DIPEA) (2.45 mL) in THF (50 mL) at 25 °C. After 2 h TLC showed complete conversion to the bis-addition product. The reaction mixture was cooled and concentrated *in vacuo*, and the residue was partitioned between EtOAc (125 mL) and brine (75 mL). The organic extract was washed with brine (70 mL), dried over $MgSO_4$, filtered, and concentrated *in vacuo* to give of the crude bis-adduct as a white solid. This bis-adduct was suspended in 1,4-dioxane (10 mL), and NH_4OH (10 mL) was added. The mixture was sealed in a Parr vessel, and the reaction stirred at 95 °C for 7 h. After cooling and depressurization, the reaction mixture was concentrated *in vacuo*, and the residue was partitioned between EtOAc (150 mL) and brine (100 mL). The organic extract was washed with brine (50 mL), dried over $MgSO_4$, filtered, and concentrated *in vacuo*. The mixture was purified by column chromatography (eluted with EtOAc) to give 1.12 g (2.89 mmol, 86%) of the product as a white solid: ^{1}H NMR (500 MHz, DMSO-d_6) δ 8.89 (s, 2 H), 7.60 (br s, 4 H), 7.23 (d, J_{ab} = 8 Hz, 4 H), 6.45 (br s, 2 H), 1.25 (s, 18 H); ^{13}C NMR (125 MHz, DMSO-d_6) δ 166.84, 164.47, 143.85, 137.46, 124.63, 120.15, 33.72, 31.17; HRMS–FAB calcd for $C_{23}H_{31}N_6$ 391.2609, found 391.2610 $(M + H)^+$.

Acknowledgment. This work was supported by The National Science Foundation (Grants CHE-91-22331 to G.M.W., DMR-89-20490 to the Harvard University Materials Research Laboratory, and CHE-80-00670 for the purchase of the Siemens X-ray diffractometer). NMR instrumentation was supported by the National Sience Foundation Grant CHE-88-14019 and the National Institutes of Health Grant 1 S10 RR4870. Mass spectrometry was performed by Dr. A. Tyler. The Harvard University Mass Spectrometry Facility was supported by The National Science Foundation Grant CHE-90-20043 and The National Institutes of Health Grant 1 S10 RR06716-01. We thank Professor Robert Cohen (MIT, Chemical Engineering) for the loan of his vapor pressure osmometer. J.P.M. was an SERC/NATO Postdoctoral Fellow, 1991–1993. C.T.S. was an Eli Lilly Predoctoral Fellow, 1991.